Inorganic Chemistry

including bioinorganic chemistry

December 15, 2014
Volume 53, Number 24
pubs.acs.org/IC

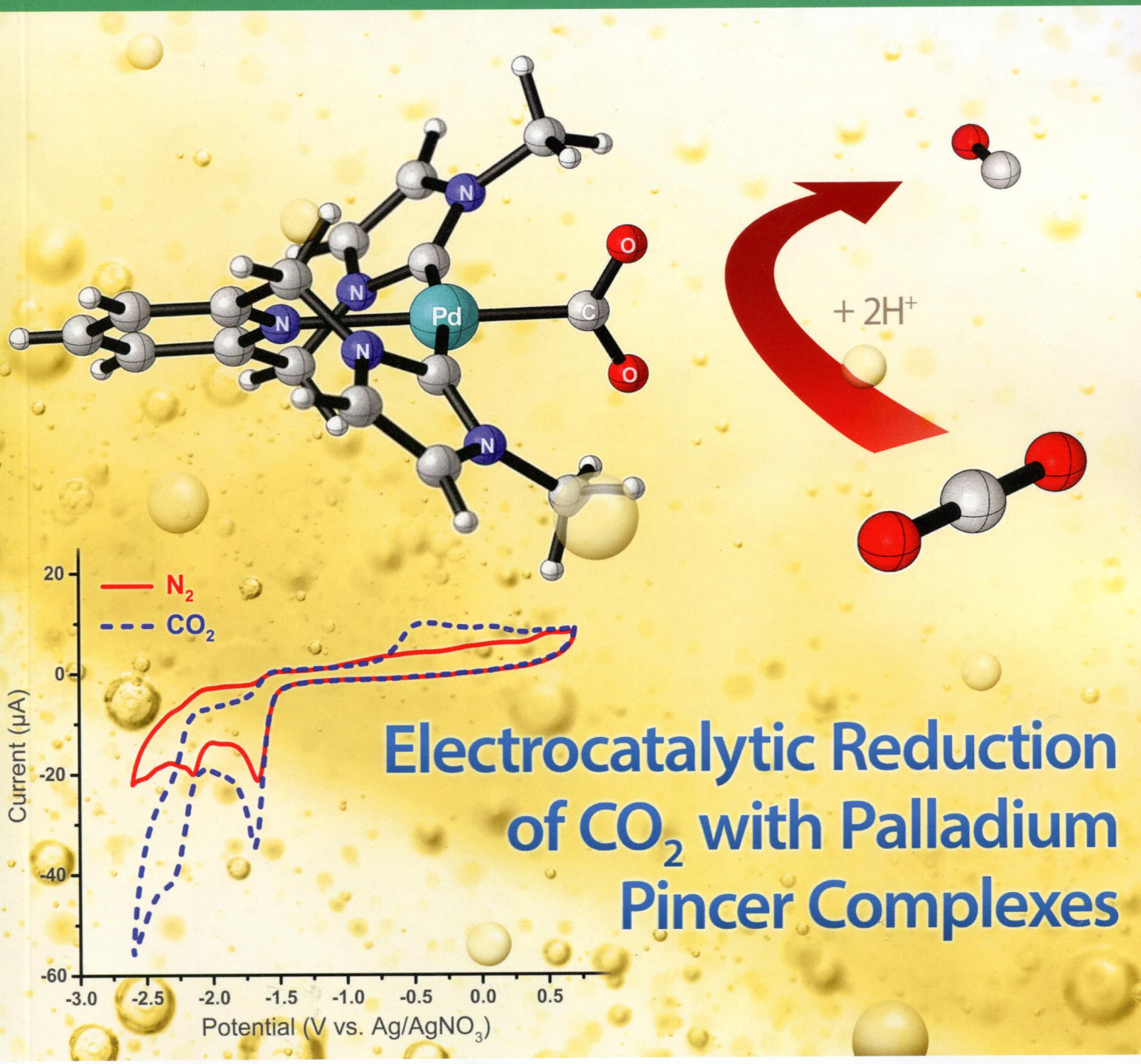

Electrocatalytic Reduction of CO_2 with Palladium Pincer Complexes

ACS Publications
Most Trusted. Most Cited. Most Read.

www.acs.org

Inorganic Chemistry

DECEMBER 15, 2014
VOLUME 53 ISSUE 24

INOCAJ 53(24) 12665−13258 (2014)
ISSN 0020-1669
Registered in the U.S. Patent and Trademark Office

ON THE COVER: Electrochemical characterization of pyridine- and lutidine-linked palladium bis-N-heterocyclic carbene pincer complexes under N_2 and CO_2 atmospheres shows that the lutidine-linked complexes electrocatalytically reduce CO_2 to CO. Comparative DFT studies of these species alongside two known CO_2 reduction electrocatalysts are used to probe CO_2-activation thermodynamics, explain varying requirements for proton sources, and investigate charge transfer from redox-active ligands. See J. A. Therrien, M. O. Wolf, and B. O. Patrick, p 12962.

Communications

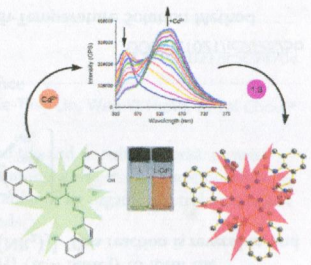

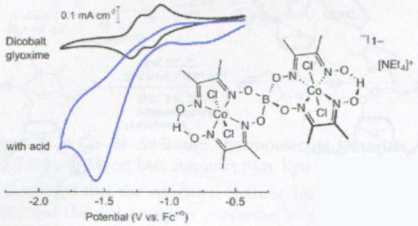

12671 S

DOI: 10.1021/ic502006s

Field-Induced Slow Magnetic Relaxation in Cobalt(II) Compounds with Pentagonal Bipyramid Geometry

Xing-Cai Huang, Chun Zhou, Dong Shao, and Xin-Yi Wang*

Three air-stable mononuclear cobalt(II) compounds with pentagonal bipyramid geometry were synthesized and magnetically characterized. Field-induced slow magnetic relaxation was observed for all of them. These are the first examples of such behavior observed in the seven-coordinated mononuclear 3d metal compounds.

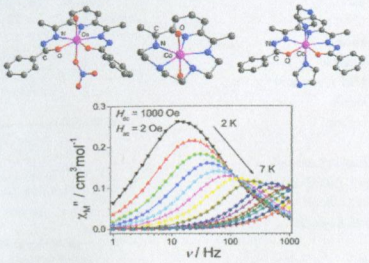

12674 S

DOI: 10.1021/ic5023642

Magnetism of Linear $[Ln_3]^{9+}$ Oxo-Bridged Clusters (Ln = Pr, Nd) Supported inside a $[R_3PR']^+$ Phosphonium Coordination Material

Nolan W. Waggoner, Beau Saccoccia, Ilich A. Ibarra, Vincent M. Lynch, Paul T. Wood,* and Simon M. Humphrey*

The magnetism of $[Ln_3]^{9+}$ clusters of Pr or Nd supported inside a coordination polymer based on organophosphonium ligands is compared to three contrasting models.

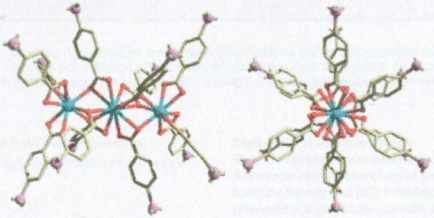

12677 S

DOI: 10.1021/ic502422u

Tetranuclear Ruthenium(II) Complex with a Dinucleating Ligand Forming Multi-Mixed-Valence States

Shingo Ohzu, Tomoya Ishizuka, Hiroaki Kotani, Yoshihito Shiota, Kazunari Yoshizawa, and Takahiko Kojima*

Stepwise chemical oxidation of a tetranuclear ruthenium(II) complex affords three different mixed-valence states, in one of which the charge is partially delocalized on the two Ru centers, to be evidenced by observation of an intervalence charge-transfer state categorized into the Robin–Day class II.

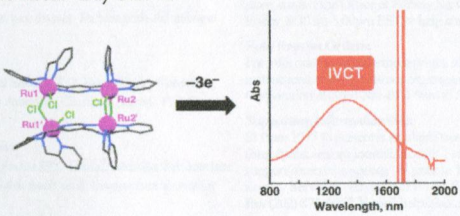

12680 S

DOI: 10.1021/ic5024357

Resolved P-Metalated Nucleoside Phosphoramidites

Erica J. Miller, Kevin J. Garcia, Erin C. Holahan, Rosa M. Ciccarelli, Rachel A. Bergin, Stephanie L. Casino, Tyler L. Bogaczyk, Michael R. Krout, Peter M. Findeis, and Robert A. Stockland Jr.*

In this Communication, we describe the synthesis of a rare class of resolved P-metalated nucleoside phosphoramidites. Although the initial compounds contained gold as the metal center, the resolved nucleoside phosphoramidites can be readily transferred to other metals.

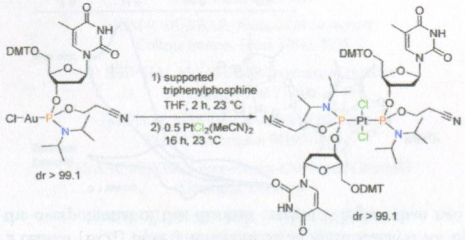

12683 S

DOI: 10.1021/ic502500z

Reversible Chalcogen-Atom Transfer to a Terminal Uranium Sulfide

Danil E. Smiles, Guang Wu, and Trevor W. Hayton*

Elemental chalcogens (S or Se) react with the terminal sulfide complex $[U(S)(NR_2)_3]$ (R = $SiMe_3$) to form the dichalcogenides $[K(18\text{-crown-6})][U(\eta^2\text{-}S_2)(NR_2)_3]$ and $[K(18\text{-crown-6})][U(\eta^2\text{-}SSe)(NR_2)_3]$. This reaction is reversible, and the addition of phosphines regenerates the terminal uranium sulfide.

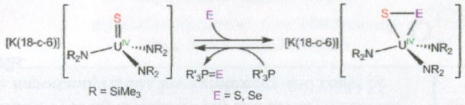

12686 S

DOI: 10.1021/ic502625b

Borate Fluoride and Fluoroborate in Alkali-Metal Borate Prepared by an Open High-Temperature Solution Method

Hongping Wu, Hongwei Yu, Qiang Bian, Zhihua Yang, Shujuan Han, and Shilie Pan*

Two novel halogen-containing borates, $Li_6RbB_2O_6F$ and $K_3B_3O_3F_6$, have been synthesized. $Li_6RbB_2O_6F$ is the first borate fluoride in alkali-metal borate. Meanwhile, $K_3B_3O_3F_6$ appears to be the first confirmed alkali-metal fluoroborate crystal grown by a high-temperature solution in air and provides the new synthesis strategy to obtain the fluoroborate crystal under ambient pressure.

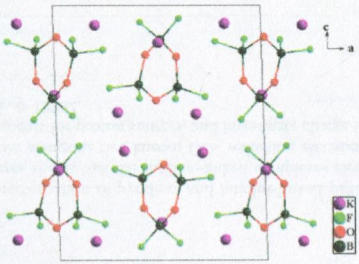

Articles

12689 S

DOI: 10.1021/ic501018a

Studies of the Pathways Open to Copper Water Oxidation Catalysts Containing Proximal Hydroxy Groups During Basic Electrocatalysis

Deidra L. Gerlach, Salome Bhagan, Alex A. Cruce, Dalton B. Burks, Ismael Nieto, Hai T. Truong, Steven P. Kelley, Corey J. Herbst-Gervasoni, Katherine L. Jernigan, Michael K. Bowman, Shanlin Pan, Matthias Zeller, and Elizabeth T. Papish*

The 2:1 complex of $[(6,6'\text{-dhbp})_2Cu]^{2+}$ has four acidic protons, and upon deprotonation with base, electrocatalytic water oxidation occurs. The proximal O- groups may help accelerate PCET events. A low overpotential of 477 mV was observed with a slow turnover rate ($k = 0.356\ s^{-1}$). This work serves to illustrate what productive (water oxidation) and nonproductive pathways are available to copper complexes of 6,6′-dhbp in basic aqueous solution under electrocatalytic conditions.

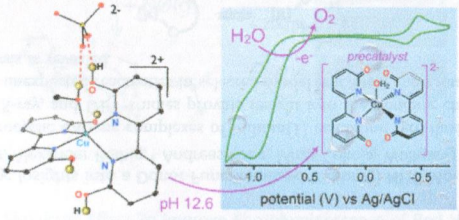

12699 S

DOI: 10.1021/ic5021065

$BaGe_6$ and $BaGe_{6-x}$: Incommensurately Ordered Vacancies as Electron Traps

Lev Akselrud, Aron Wosylus, Rodrigo Castillo, Umut Aydemir, Yurii Prots, Walter Schnelle, Yuri Grin, and Ulrich Schwarz*

We report two new phases in the system Ba−Ge synthesized at high-pressure high-temperature conditions: $BaGe_6$ comprising a three-dimensional germanium framework and its defect variant $BaGe_{5.5}$. The germanium-deficient compound adopts a motif with incommensurate modulations requiring a four-dimensional description of the atomic pattern. Quantum chemical bonding analysis reveals that the fragmentation of the catena-type building units induces the formation of electron pairs around the voids thus causing a semiconductor-type electron balance.

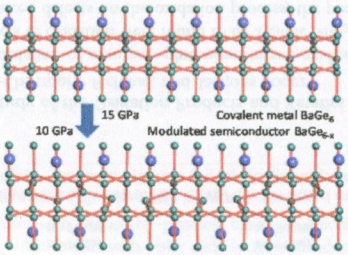

12706 DOI: 10.1021/ic501259g

Synthesis, Spectral, and Electrochemical Studies of Electronically Tunable *β*-Substituted Porphyrins with Mixed Substituent Pattern

Ravi Kumar and Muniappan Sankar*

Two new families of mixed substituted porphyrins, viz. 2-nitro-12,13-disubstituted-*meso*-tetraphenylporphyrins (H_2TPP-(NO_2)X_2, X = Ph, phenylethynyl (PE), 2-thienyl (Th), Br, and CN) and 2-nitro-7,8,12,13,17,18-hexasubstituted-*meso*-tetraphenylporphyrins (H_2TPP(NO_2)X_6, X = Br, Ph, PE, and Th), and their metal (Co(II), Ni(II), Cu(II), and Zn(II)) complexes have been synthesized. H_2TPP(NO_2)X_6 exhibited a dramatic red shift in the electronic spectral features, significant downfield resonances of the core imino protons, higher protonation/deprotonation constants, and tunable electrochemical redox properties with a considerable reduction in the HOMO−LUMO gap which are interpreted in terms of a combined effect of nonplanarity and/or the electronic effect of the substituents.

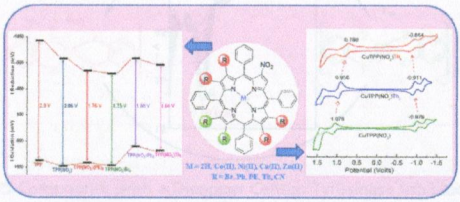

12720 DOI: 10.1021/ic501470v

Tetragold(I) Complexes: Solution Isomerization and Tunable Solid-State Luminescence

Thuy Minh Dau, Yi-An Chen, Antti J. Karttunen, Elena V. Grachova, Sergey P. Tunik,* Ke-Ting Lin, Wen-Yi Hung, Pi-Tai Chou,* Tapani A. Pakkanen, and Igor O. Koshevoy*

The tetragold(I) clusters supported by the triphosphine ligand adopt two structural motifs and in solution exist as two isomeric species in slow chemical equilibria. In the solid state, the title complexes exhibit moderate-to-strong phosphorescence, exhibiting quantum yields up to 51%. Decent quantum efficiency allowed for the fabrication of an organic electroluminescent device, which has been achieved for the first time using polynuclear gold(I) compounds.

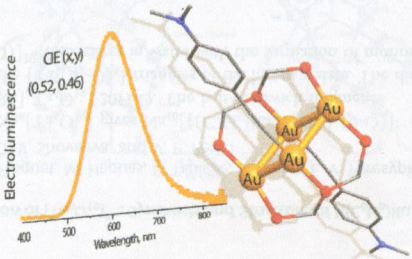

12732 DOI: 10.1021/ic5014945

Effects of Doping on Transport Properties in Cu−Bi−Se-Based Thermoelectric Materials

Jae-Yeol Hwang, Hyeon A. Mun, Sang Il Kim, Ki Moon Lee, Jungeun Kim, Kyu Hyoung Lee,* and Sung Wng Kim*

On the basis of structural analysis, it is verified that the structural features, including atomic bonding and configurations, are strongly correlated with both electronic and thermal transport properties in the pavonite homologue $Cu_{x+y}Bi_{5-y}Se_8$ system. Extremely low lattice thermal conductivity of 0.32 W m^{-1} K^{-1} was achieved at 560 K by Zn doping at interstitial Cu site.

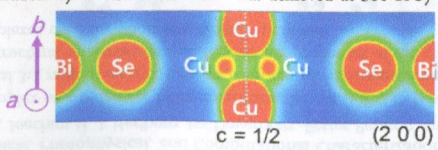

12739 Ⓢ DOI: 10.1021/ic501566u

Synthesis, Structure, and Optical Properties of Pt(II) and Pd(II) Complexes with Oxazolyl- and Pyridyl-Functionalized DPPM-Type Ligands: A Combined Experimental and Theoretical Study

Shuanming Zhang, Roberto Pattacini, Pierre Braunstein,* Luisa De Cola,* Edward Plummer, Matteo Mauro, Christophe Gourlaouen, and Chantal Daniel*

The structural and optical properties of newly synthesized and characterized divalent Pt(II) and Pd(II) complexes featuring oxazolyl- and pyridyl-functionalized diphenylphosphinomethanide ligands are discussed on the basis of a joint experimental/theoretical study. The possibility to stabilize tautomeric forms of functional diphosphine ligands by metal coordination is demonstrated. The versatility of these functional ligands suggests that the bonding rearrangements are more complex than anticipated. Coordination of the free ligands to the metal cations completely modifies the optical properties.

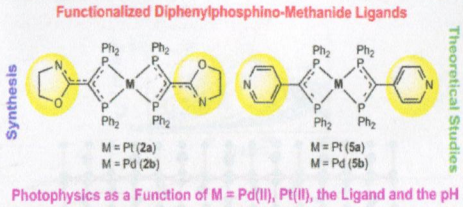

12757 DOI: 10.1021/ic501580x

High Temperature X-ray Diffraction Study of the Oxidation Products and Kinetics of Uranium–Plutonium Mixed Oxides

Michal Strach,* Renaud C. Belin,* Jean-Christophe Richaud, and Jacques Rogez

The phenomena taking place during oxidation of uranium–plutonium mixed oxides affect the long-range ordering in the structure of these materials. The products of oxidation were found to be a cubic MO_{2+x} and a hexagonal M_3O_8 structures. We discuss the effect of self-irradiation induced defects on the oxidation process, the possibility of cation migration between the two structures, and the limits of solubility of Pu in M_3O_8 and oxygen in MO_{2+x}.

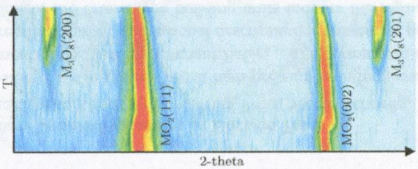

12767 Ⓢ DOI: 10.1021/ic5016324

On the Concept of Hemilability: Insights into a Donor-Functionalized Iridium(I) NHC Motif and Its Impact on Reactivity

Korbinian Riener, Mario J. Bitzer, Alexander Pöthig,* Andreas Raba, Mirza Cokoja, Wolfgang A. Herrmann, and Fritz E. Kühn*

N-donor-functionalized N-heterocyclic carbene complexes of iridium(I) exhibiting rare fluxional coordination behavior are presented. Detailed VT-NMR, X-ray, and DFT studies provide insight into the bonding characteristics of these hemilabile systems. The compounds show unexpected reactivities in selected model reactions, and remarkable activity as well as stability in transfer-hydrogenation catalysis is revealed.

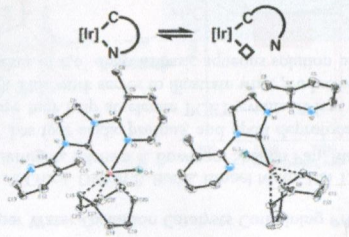

12778 S DOI: 10.1021/ic502432c

A Homoleptic Trisbidentate Ru(II) Complex of a Novel Bidentate Biheteroaromatic Ligand Based on Quinoline and Pyrazole Groups: Structural, Electrochemical, Photophysical, and Computational Characterization

Martin Jarenmark, Lisa A. Fredin, Joachim H. J. Hedberg, Isa Doverbratt, Petter Persson, and Maria Abrahamsson*

The first homoleptic Ru(II) complex of a bidentate biheteroaromatic ligand (QPzH) based on an 8-quinolinyl motif was synthesized. Thermally a statistical 3:1 ratio of *mer*/*fac* isomers is produced, but exposure to visible light makes isolation of the pure *mer* isomer possible. The structural, spectroscopic, and electronic properties of the complex are evaluated and discussed in relation to other Ru(II) complexes used for photosensitization purposes.

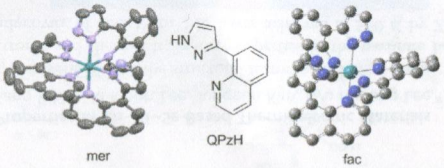

12791 S DOI: 10.1021/ic501622t

Coordination-Induced Condensation of $[Ta_6O_{19}]^{8-}$: Synthesis and Structure of $[\{(C_6H_6)Ru\}_2Ta_6O_{19}]^{4-}$ and $[\{(C_6H_6)RuTa_6O_{18}\}_2(\mu\text{-}O)]^{10-}$

P. A. Abramov, M. N. Sokolov,* S. Floquet, M. Haouas, F. Taulelle, E. Cadot, E. V. Peresypkina, A. V. Virovets, C. Vicent, N. B. Kompankov, A. A. Zhdanov, O. V. Shuvaeva, and V. P. Fedin

Reaction of $[(C_6H_6)RuCl_2]_2$ and $Na_8[Ta_6O_{19}]$ gives $Na_{10}[\{(C_6H_6)RuTa_6O_{18}\}_2(\mu\text{-}O)]\cdot 39.4H_2O$ and $Na_4(trans\text{-}[\{(C_6H_6)Ru\}_2Ta_6O_{19}]\cdot 20H_2O$. The half-sandwich fragments $\{(C_6H_6)Ru\}^{2+}$ are coordinated to the $\{Ta_3(\mu_2\text{-}O)_3\}$ triangles of the hexatantalate. The dimeric complex $[\{(C_6H_6)RuTa_6O_{18}\}_2(\mu\text{-}O)]^{10-}$ dissociates in water with the formation of monomeric $[(C_6H_6)RuTa_6O_{19}]^{6-}$ species.

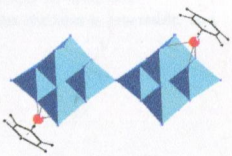

12799 S DOI: 10.1021/ic501742j

One Electron Reduced Square Planar Bis(benzene-1,2-dithiolato) Copper Dianionic Complex and Redox Switch by O_2/HO^-

Biplab K. Maiti, Luisa B. Maia, Kuntal Pal, Bholanath Pakhira, Teresa Avilés,* Isabel Moura, Sofia R. Pauleta, José L. Nuñez, Alberto C. Rizzi, Carlos D. Brondino,* Sabyasachi Sarkar,* and José J. G. Moura*

Bis(benzene-1,2-dithiolato)copper complexes $\mathbf{1}^{red}$ and $\mathbf{1}^{ox}$ can be interconverted in the presence of O_2 or base (Et_4NOH) respectively. EPR measurements and DFT calculations on the reduced form ($\mathbf{1}^{red}$) show a strong covalency of the Cu–S bonds with high electron density on the sulfur atoms. These results provide new information to the chemistry of copper ions in sulfur rich environments.

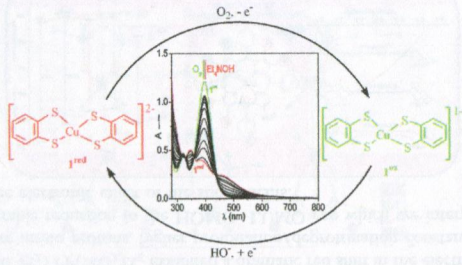

12809 S DOI: 10.1021/ic501765g

Synthesis of Bis(imidazole) Metal Complexes and Their Use in Rapid NO Detection and Quantification Devices
Eric Victor, Sunghee Kim, and Stephen J. Lippard*

A series of colorimetric sensors were developed with the motif $M(BIPhMe)X_2$. The reactivity of these complexes toward $NO(g)$ and $NO_2(g)$ in solution was explored and characterized. These complexes were then incorporated into test strips and syringes to provide devices that can qualitatively, and in the case of the syringes quantitatively, detect $NO(g)$ and $NO_2(g)$ in a reaction headspace without additional equipment.

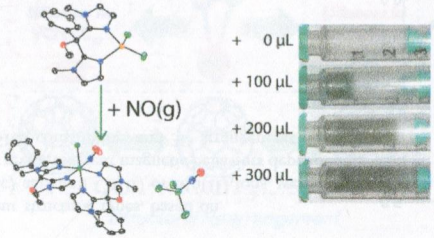

12822 S DOI: 10.1021/ic5017752

Domination of Second-Sphere Shrinkage Effect To Improve Photoluminescence of Red Nitride Phosphors
Wan-Yu Huang, Fumitaka Yoshimura, Kyota Ueda, Wei Kong Pang, Bing-Jian Su, Ling-Yun Jang, Chang-Yang Chiang, Wuzong Zhou, Nguyen Hoang Duy, and Ru-Shi Liu*

Promising red nitride phosphors with higher eye sensitivity and thermal stability are obtained by varying nonactivator sites of the second sphere in $CaAl_{1-4\delta/3}Si_{1+\delta}N_3:Eu^{2+}$ ($\delta = 0.345$). Emission and thermal stability are dominated by the second-sphere shrinkage effect through controlling local environments of the $Ca_{0.99}Al_{1-4\delta/3-x}Si_{1+\delta+x}N_{3-x}C_x:Eu^{2+}_{0.01}$ system.

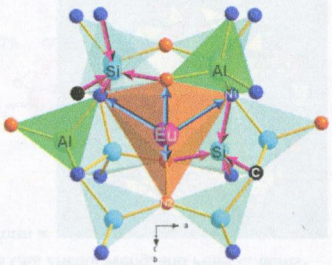

12832 S DOI: 10.1021/ic501794z

Oxorhenium(V) Complexes with Phenolate–Pyrazole Ligands for Olefin Epoxidation Using Hydrogen Peroxide
Niklas Zwettler, Jörg A. Schachner, Ferdinand Belaj, and Nadia C. Mösch-Zanetti*

The synthesis of oxorhenium(V) complexes with phenolate–pyrazole ligands is described. The effects of polarity and electron-withdrawal were studied by introducing substitutents with polar and electron-withdrawing groups (R = NO_2, Br) and a polar-only group (R = OMe). These complexes are rare examples of Re(V) complexes that are able to epoxidize cyclooctene using hydrogen peroxide instead of *tert*-butylhydroperoxide. Also, these complexes are active epoxidation catalysts in green solvents such as diethylcarbonate.

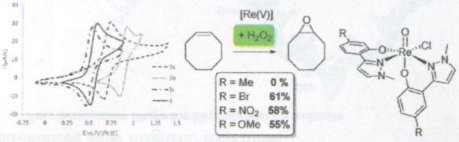

12841 S DOI: 10.1021/ic501812n

Single-Crystalline Organic–Inorganic Layered Cobalt Hydroxide Nanofibers: Facile Synthesis, Characterization, and Reversible Water-Induced Structural Conversion

Xiaodi Guo, Lianying Wang,* Shuang Yue, Dongyang Wang, Yanluo Lu, Yufei Song, and Jing He

Single-crystalline organic–inorganic layered cobalt hydroxide nanofibers intercalated with benzoate ions $[Co(OH)(C_6H_5COO)\cdot H_2O]$ have been controllably synthesized by a simple self-assembly process in water. They are of high quality in terms of morphology, size, uniformity, crystallinity, and purity, and have been well-characterized with various tools. A coordination-driven mechanism is proposed for their anisotropic growth. More importantly, the resulting nanofibers exhibit a reversible transformation involving the loss and reuptake of unusually weakly coordinated water molecules.

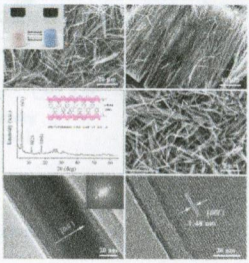

12848 S DOI: 10.1021/ic501829s

Exploring the Interaction of N/S Compounds with a Dicopper Center: Tyrosinase Inhibition and Model Studies

Elina Buitrago, Alexandra Vuillamy, Ahcène Boumendjel, Wei Yi, Gisèle Gellon, Renaud Hardré, Christian Philouze, Guy Serratrice, Hélène Jamet, Marius Réglier,* and Catherine Belle*

We report a full description at the enzymatic level of phenylmethylene thiosemicarbazone (PTSC) and phenylthiourea (PTU), as inhibitors of Tyrosinase (Ty). Both compounds exhibit competitive inhibition. With a K_{IC} value of 0.93 μM, PTSC is one of the best mushroom Ty inhibitors. Binding studies with PTU and PTSC on a dicopper complex reminiscent of the active site of tyrosinase are presented and X-ray crystal structures evidence that PTU and PTSC bind as bridged, bidentate, and monodeprotonated ligands.

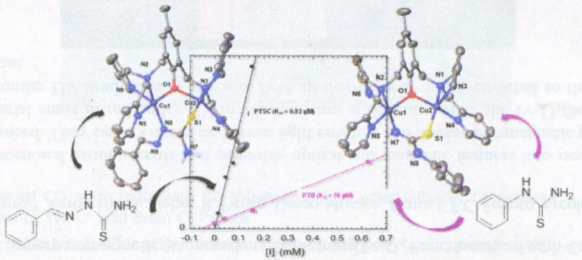

12859 S DOI: 10.1021/ic501869y

Reasons behind the Relative Abundances of Heptacoordinate Complexes along the Late First-Row Transition Metal Series

Martín Regueiro-Figueroa, Luís M. P. Lima, Víctor Blanco, David Esteban-Gómez, Andrés de Blas, Teresa Rodríguez-Blas, Rita Delgado, and Carlos Platas-Iglesias*

A detailed analysis of the structure of seven-coordinate $[ML^1]$ complexes (M = Co, Ni, Cu, or Zn) shows that an unfavorable distribution of the metal 3d electrons of Ni^{2+} is responsible for the unusual stability trend observed for these complexes ($Co^{2+} > Ni^{2+} < Cu^{2+} > Zn^{2+}$), and explains why seven-coordinate complexes of Ni are particularly rare.

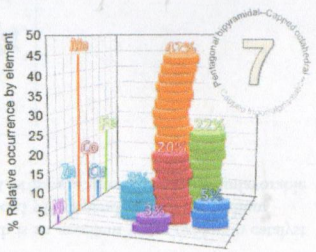

12870 S

DOI: 10.1021/ic501870h

Supramolecular Control over Molecular Magnetic Materials: γ-Cyclodextrin-Templated Grid of Cobalt(II) Single-Ion Magnets

Natalia Nedelko, Arkadiusz Kornowicz, Iwona Justyniak, Pavlo Aleshkevych, Daniel Prochowicz, Piotr Krupiński, Orest Dorosh, Anna Ślawska-Waniewska,* and Janusz Lewiński*

γ-Cyclodextrin was used to template magnetic Co^{II} and nonmagnetic auxiliary Li^{+} ions to form a heterometallic $\{Co, Li, Li\}_4$ ring. In the sandwich-type complex $[(\gamma\text{-CD})_2Co_4Li_8(H_2O)_{12}]$ spatially separated Co^{II} ions are prevented from superexchange magnetic coupling and reveal field-induced slow magnetic relaxations.

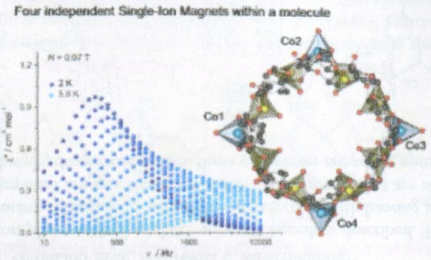

12877 S

DOI: 10.1021/ic5018449

Hybrid Uranium–Transition-Metal Oxide Cage Clusters

Jie Ling, Franklin Hobbs, Steven Prendergast, Pius O. Adelani, Jean-Marie Babo, Jie Qiu, Zhehui Weng, and Peter C. Burns*

Uranyl, phosphate, and tungstate/molybdate self-assemble in aqueous solution to form a family of complex nanoscale actinide-transition-metal hybrid polyoxometalates.

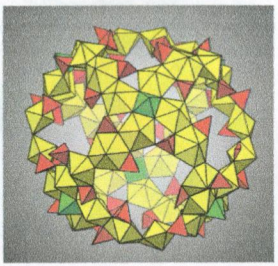

12885 S

DOI: 10.1021/ic501898x

Unusual Magnetic Behaviors and Electronic Configurations Driven by Diverse Co(II) or Mn(II) MOF Architectures

María Celeste Bernini, Julio Romero de Paz, Natalia Snejko, Regino Sáez-Puche, Enrique Gutierrez-Puebla, and María Ángeles Monge*

Five novel MOFs belonging to four structural types, based on hexafluorisopropylidenebis(benzoic) acid and Co(II) or Mn(II) ions, were obtained. Magnetic measurements reveal different magnetic behaviors dependent on the coordination geometries, SBU constitution, and 3D arrangement of the magnetic atoms.

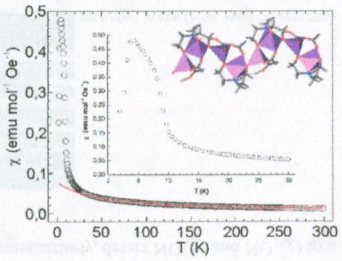

12896 S DOI: 10.1021/ic501894u

Ligand Exchange and Redox Processes in Iridium Triazolylidene Complexes Relevant to Catalytic Water Oxidation

Ana Petronilho, Antoni Llobet,* and Martin Albrecht*

Investigation of the reactivity patterns of a triazolylidene iridium aqua complex, which is an excellent water oxidation catalyst precursor, indicates a relatively low pK_a of the metal-bound aqua ligand, a pronounced pH dependence of the iridium oxidation potential, and selective ligand exchange reactions. Cosolvents such as MeCN have a pronounced and unfavorable impact on the oxidation potential.

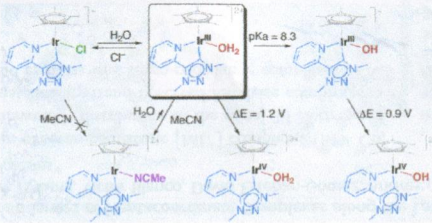

12902 S DOI: 10.1021/ic5018856

Red-Green Emitting and Superparamagnetic Nanomarkers Containing Fe_3O_4 Functionalized with Calixarene and Rare Earth Complexes

Latif U. Khan, Hermi F. Brito,* Jorma Hölsä, Kleber R. Pirota, Diego Muraca, Maria C.F.C. Felinto, Ercules E.S. Teotonio, and Oscar L. Malta

Novel sophisticated, bifunctional nanomaterials that assemble optical and magnetic features into new single discrete entity nanoparticle were synthesized. They can act as red and green light emitters and display paramagnetic properties. The Fe_3O_4@calix-Eu(TTA) nanomaterial emits in red under UV irradiation lamp at 365 nm, while the Fe_3O_4@calix-Tb(ACAC) one displays green emission under UV irradiation at 254 nm. Both of them can be easily attracted to the external magnet in suspension and solid phase.

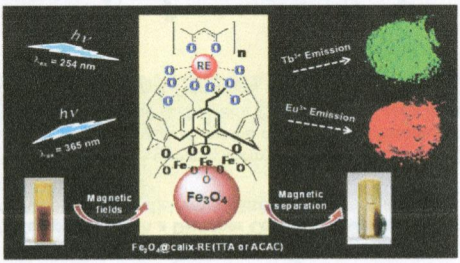

12911 S

DOI: 10.1021/ic501911z

Quantum Chemical Determination of Novel C_{82} Monometallofullerenes Involving a Heterogeneous Group

Hong Zheng, Xiang Zhao,* Ling He, Wei-Wei Wang, and Shigeru Nagase

Isomorphous YCN@C_{82} and TbCN@C_{82} species including novel triangular heterogeneous metalloclusters are determined to be of different thermodynamic stabilities and complicated electronic features by means of quantum chemical characterizations combined with statistical thermodynamic analyses.

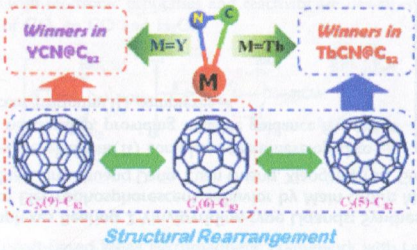

12918 S

DOI: 10.1021/ic501932c

Oxorhenium(V) Complexes with Phenolate–Oxazoline Ligands: Influence of the Isomeric Form on the O-Atom-Transfer Reactivity

Jörg A. Schachner, Belina Terfassa, Lydia M. Peschel, Niklas Zwettler, Ferdinand Belaj, Pawel Cias, Georg Gescheidt, and Nadia C. Mösch-Zanetti*

Two coordination isomers **3a** and **3a′** of an oxorhenium(V) complex equipped with two bidentate phenolate–oxazoline ligands have been fully characterized and tested in the catalytic reduction of perchlorates. In contrast to previously published isomer **3a** (*N*,*N*-trans), the previously unknown *N*,*N*-cis isomer **3a′** shows a significantly lower catalytic activity in perchlorate reduction (16 vs 87%; 3.2 mol % catalyst loading, 20 °C). Experimental as well as theoretical results are presented to explain this large difference in the observed catalytic activity.

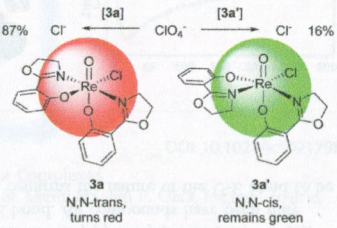

12929 S

DOI: 10.1021/ic501951f

Building Complexity in O_2-Binding Copper Complexes. Site-Selective Metalation and Intermolecular O_2-Binding at Dicopper and Heterometallic Complexes Derived from an Unsymmetric Ligand

Joan Serrano-Plana, Miquel Costas,* and Anna Company*

An unsymmetric ligand (L^{N3N4}) linking tridentate and a tetradentate binding sites by a *m*-xylyl spacer was synthesized to prepare homo- and dimetallic complexes, where each metal ion binds in a unique environment. Reaction of the heterodimetallic complexes $[CuM'(L^{N3N4})]^{n+}$ (M′ = Cu^{I}, Zn^{II}, Fe^{II}, Cu^{II}, or Ga^{III}) with O_2 at low temperature is used to determine the final position of the Cu^{I} center in the system because only one Cu_2O_2 species is formed.

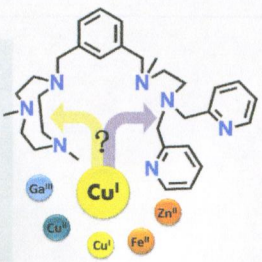

12939 Ⓢ DOI: 10.1021/ic502024a

Tuning the Selectivity of Gd_3N Cluster Endohedral Metallofullerene Reactions with Lewis Acids

Steven Stevenson,* Khristina A Rottinger, Muska Fahim, Jessica S Field, Benjamin R Martin, and Kristine D Arvola

The reactivity of Lewis acids with Gd_3N endohedrals can be tuned to selectively fractionate them from complex mixtures. The order of increasing reactivity and decreasing selectivity (left to right) is as follows: $CaCl_2 < ZnCl_2 < NiCl_2 < MgCl_2 < MnCl_2 < CuCl_2 < WCl_4 \ll WCl_6 < ZrCl_4 < AlCl_3 < FeCl_3$. The ability to now control metallofullerene precipitation is a significant outcome of this work.

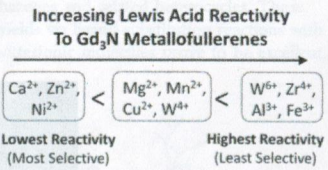

12947 Ⓢ DOI: 10.1021/ic5020362

Dual Emission and Excited-State Mixed-Valence in a Quasi-Symmetric Dinuclear Ru–Ru Complex

Christoph Kreitner, Markus Grabolle, Ute Resch-Genger, and Katja Heinze*

The bimetallic dipeptide $[(EtOOC\text{-}tpy)Ru(tpy\text{-}NHCO\text{-}tpy)Ru(tpy\text{-}NHCOCH_3)]^{4+}$ shows dual emission in fluid solution at room temperature arising from two equilibrating triplet states centered on the C- and N-terminal ruthenium sites. The Ru^{II} and Ru^{III} centers in these triplet valence isomers are electronically coupled through a bridging radical anion. In contrast the mixed-valent complex $[(EtOOC\text{-}tpy)Ru(tpy\text{-}NHCO\text{-}tpy)Ru(tpy\text{-}NHCOCH_3)]^{5+}$ with a neutral bridging ligand is valence-localized. The equilibrating excited triplet states can be reduced by $PhNMe_2$ via a N···HN hydrogen bridge.

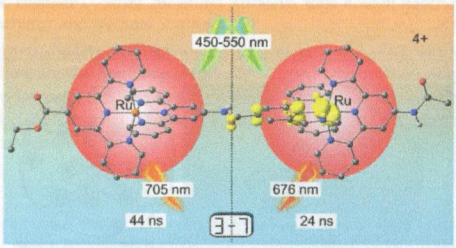

12962 Ⓢ DOI: 10.1021/ic502056w

Electrocatalytic Reduction of CO_2 with Palladium Bis-N-heterocyclic Carbene Pincer Complexes

Jeffrey A. Therrien, Michael O. Wolf,* and Brian O. Patrick

A series of pyridine- and lutidine-linked bis-NHC palladium pincer complexes are screened as CO_2 reduction electrocatalysts, with the lutidine-linked complexes displaying homogeneous electrocatalytic capabilities at potentials as low as −1.6 V versus $Ag/AgNO_3$. DFT studies indicate redox activity of the ligand, contributing to stability of the reduced species and potentially addressing a major deactivation pathway of previous palladium pincer CO_2 reduction electrocatalysts.

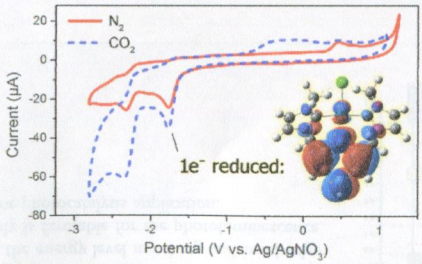

12973 S

DOI: 10.1021/ic5020829

Multifunctional Anionic MOF Material for Dye Enrichment and Selective Sorption of C_2 Hydrocarbons over Methane via Ag^+-Exchange

Yan-Xi Tan, Ying Zhang,* Yan-Ping He, Yan-Jun Zheng, and Jian Zhang*

Presented here is a multifunctional anionic MOF material that can upgrade selective sorption of C_2s/C_1 via Ag^+-exchange and act as substrate to load fluorescent dyes on the external surface of crystals to control their luminescent properties.

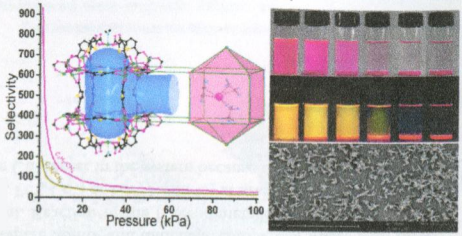

12977 S

DOI: 10.1021/ic5020658

Trivalent Uranium Phenylchalcogenide Complexes: Exploring the Bonding and Reactivity with CS_2 in the Tp*$_2$UEPh Series (E = O, S, Se, Te)

Ellen M. Matson, Andrew T. Breshears, John J. Kiernicki, Brian S. Newell, Phillip E. Fanwick, Matthew P. Shores, Justin R. Walensky,* and Suzanne C. Bart*

The trivalent uranium phenylchalcogenide series, Tp*$_2$UEPh (Tp* = hydrotris(3,5-dimethylpyrazolyl)borate, E = O (**1**), S (**2**), Se (**3**), Te (**4**)), has been synthesized to investigate the nature of the U−E bond. All compounds have been fully characterized by structural and spectroscopic methods. A computational analysis confirms the nature of the U-E bond to be primarily ionic with a small covalent contribution.

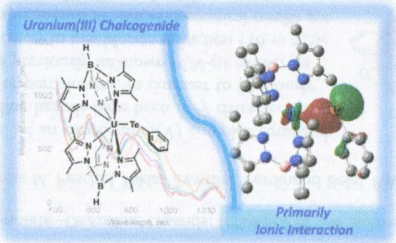

12986 S

DOI: 10.1021/ic502122t

Phosphorescent Platinum(II) Complexes Bearing 2-Vinylpyridine-type Ligands: Synthesis, Electrochemical and Photophysical Properties, and Tuning of Electrophosphorescent Behavior by Main-Group Moieties

Xiaolong Yang, Xianbin Xu, Jiang Zhao, Jing-shuang Dang, Zuan Huang, Xiaogang Yan, Guijiang Zhou,* and Dongdong Wang*

Deep red-emitting 2-vinylpyridine-type platinum(II) complexes were developed to establish their structure−property relationship, providing valuable guidance for design and synthesis of new phosphorescent platinum(II) complexes.

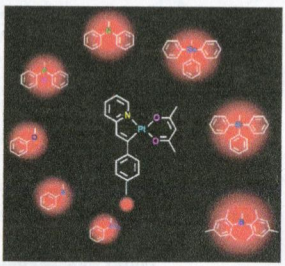

13001 DOI: 10.1021/ic5021059

Structural, Electronic, and Optical Properties of Eu-Doped BiOX (X = F, Cl, Br, I): A DFT+U Study

Zong-Yan Zhao* and Wen-Wu Dai

There is an isolated Eu-4f impurity energy band in the middle of the band gaps of BiOX. Furthermore, Eu doping enhances the internal electric fields of BiOXs and makes the variation of band gaps and band widths become more outstanding. Taking into account the energy level matching and band edge position, Eu-doped BiOCl not only is favorable for the photoluminescence application but also is favorable for photocatalysis application.

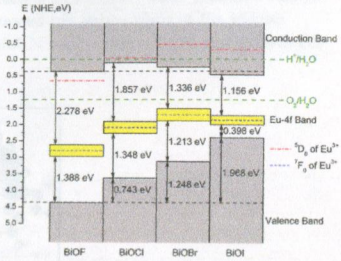

13012 DOI: 10.1021/ic502144z

Luminescent Hydrogel Particles Prepared by Self-Assembly of β-Cyclodextrin Polymer and Octahedral Molybdenum Cluster Complexes

Kaplan Kirakci,* Václav Šícha, Josef Holub, Pavel Kubát, and Kamil Lang*

Self-assembly between polymeric β-cylodextrin and octahedral molybdenum cluster complexes provides luminescent hydrogel particles useful for oxygen sensing and singlet oxygen production in water.

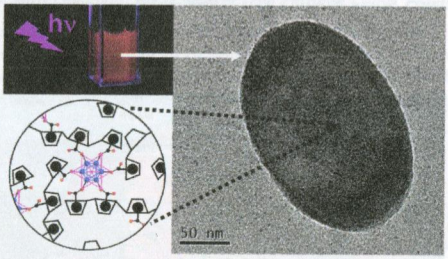

13019 DOI: 10.1021/ic5021548

Mixed Ligand $Cu^{II}N_2O_2$ Complexes: Biomimetic Synthesis, Activities in Vitro and Biological Models, Theoretical Calculations

Chen Li, Bing Yin, Yifan Kang, Ping Liu,* Liang Chen, Yaoyu Wang, and Jianli Li*

New $Cu^{II}N_2O_2$ complexes, which were obtained based on biomimetic synthesis strategy, exerted effective superoxide dismutase activity and catecholase activity. From the perspective of the complex outer sphere, the structure–activity relationship of these complexes was investigated by an experimental and computational approach. These complexes possess potent intracellular antioxidant capacity and favorable biocompatibility, suggesting their promising application potential.

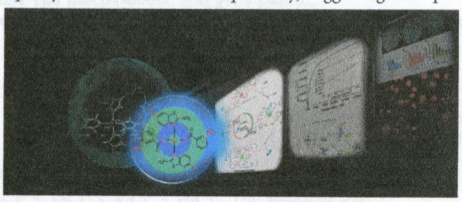

13031 S

DOI: 10.1021/ic5021725

Reactivity of a Series of Isostructural Cobalt Pincer Complexes with CO_2, CO, and H^+

David W. Shaffer, Samantha I. Johnson, Arnold L. Rheingold, Joseph W. Ziller, William A. Goddard III, Robert J. Nielsen, and Jenny Y. Yang*

A series of isostructural cobalt pincer complexes $\{Co[(t\text{-bu})_2P^EPy^EP(t\text{-bu})_2]\}^{2+}$, with Py = pyridine, E = CH_2, NH, O, and their reactivity upon reduction with the substrates CO_2, CO, and H^+ are described using experimental and quantum mechanical methods. Correlations with electronic properties and reactivity are described in the context of rational catalyst design for the selective reduction of CO_2 to CO and H_2O.

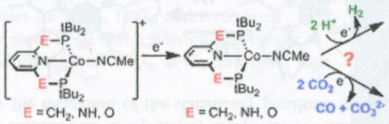

13042 S

DOI: 10.1021/ic502177k

Design and Synthesis of Stable Cobalt-Based Weak Ferromagnetic Framework with Large Spin Canting Angle

Ting Liu, Su-Mei Gao, Long-Yang Xu, Jiong-Peng Zhao,* Fu-Chen Liu,* Hai-Liang Hu, and Zhen-Hui Kang*

The stable cobalt-based framework-structured complex was synthesized which exhibits weak ferromagnetism with T_N about 4.0 K and big canting angle of 14.8°.

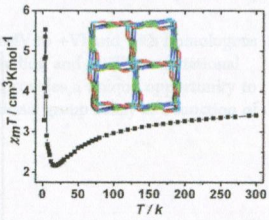

13049 S

DOI: 10.1021/ic502179f

Dual Charge-Transfer in Rhenium(I) Thioether Substituted Hexaazanaphthalene Complexes

Holly van der Salm, Michael G. Fraser, Raphael Horvath, Jack O. Turner, Gregory M. Greetham, Ian P. Clark, Michael Towrie, Nigel T. Lucas, Michael W. George,* and Keith C. Gordon*

Mono-, bi-, and trinuclear rhenium(I) complexes of hexaazanaphthalene with thioether substituents are prepared and characterized. These have intense visible absorptions due to metal-to-ligand and intraligand charge transfer.

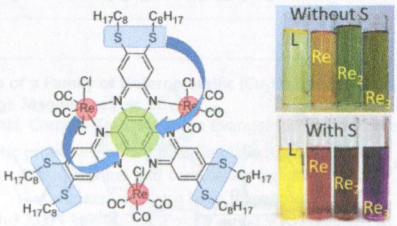

13061 Ⓢ DOI: 10.1021/ic502229w

Low-Valent Chemistry: An Alternative Approach to Phosphorus-Containing Oligomers

Stephanie C. Kosnik, Gregory J. Farrar, Erin L. Norton, Benjamin F. T. Cooper, Bobby D. Ellis, and Charles L. B. Macdonald*

We present a convenient preparation of phosphorus-rich analogues of polyphosphazenes and related heterocycles. These oligomers, all of which contain multiple P^I fragments, are synthesized in excellent yields via ligand-substitution reactions with bis(phosphine) ligands and a triphosphenium P^I precursor. Furthermore, these zwitterionic molecules prove to be excellent multidentate ligands for univalent coinage metals.

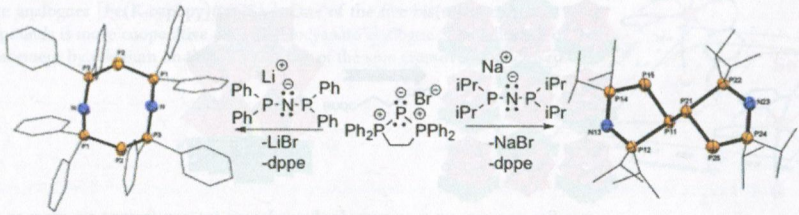

13070 Ⓢ DOI: 10.1021/ic502215h

Spin Crossover in Tetranuclear Fe(II) Complexes, $\{[(tpma)Fe(\mu\text{-}CN)]_4\}X_4$ ($X = ClO_4^-$, BF_4^-)

Oleksandr Hietsoi, Paul W. Dunk, Heather D. Stout, Alejandra Arroyave, Kirill Kovnir, Raechel E. Irons, Nazira Kassenova, Rakhmetulla Erkasov, Catalina Achim,* and Michael Shatruk*

Fe(II) precursors capped with a tetradentate tris(2-pyridylmethyl)amine ligand react with cyanide anions to afford CN-bridged tetranuclear clusters. These are the first "homoleptically" capped tetranuclear complexes that exhibit spin-crossover behavior. The high-spin (HS) to low-spin (LS) conversion is more abrupt and complete for the crystals kept under mother liquor than for the dried crystals. The observed behavior has been attributed to the increased structural disorder and lower cooperativity of the spin-state conversion in the dried samples.

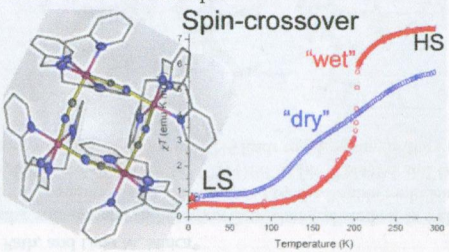

13078 DOI: 10.1021/ic502251p

Synthesis, Characterization, and Reactivity of Iron(III) Complexes Supported by a Trianionic ONO^{3-} Pincer Ligand

Matias E. Pascualini, Natali V. Di Russo, Pedro A. Quintero, Annaliese E. Thuijs, Dawid Pinkowicz, Khalil A. Abboud, Kim R. Dunbar, George Christou, Mark W. Meisel, and Adam S. Veige*

A family of Fe(III) complexes supported by the trianionic pincer-type ligand $[CF_3{-}ONO]^{3-}$ are prepared and characterized by NMR spectroscopy, single-crystal X-ray crystallography, EPR spectroscopy, SQUID magnetometry, cyclic voltammetry, and combustion analysis.

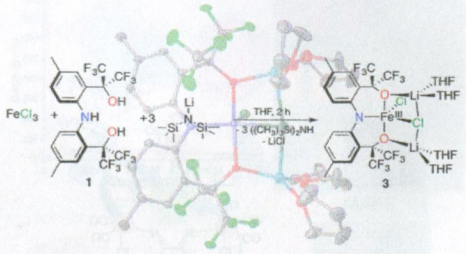

13089 DOI: 10.1021/ic502192h

Synthesis, Structural, and Transport Properties of Cr-Doped $BaTi_2As_2O$

Qiucheng Ji, Yonghui Ma, Kangkang Hu, Bo Gao, Gang Mu,* Wei Li, Tao Hu, Ganghua Zhang, Qingbiao Zhao, Hui Zhang, Fuqiang Huang, and Xiaoming Xie

The crystal structure of $BaTi_2As_2O$ is composed of edge-shared $[Ti_2As_2O]$ layers separated by the layers of Ba^{2+}. The conductive $[Ti_2Pn_2O]$ layer has a Ti_2O square net with an anti-CuO_2-type structure, where the Pn atoms are located above and below the Ti_2O squares. Cr elements are substituted into the crystal successfully, which suppress the transition temperature of the charge density wave ordering. No superconductivity is observed down to 2 K.

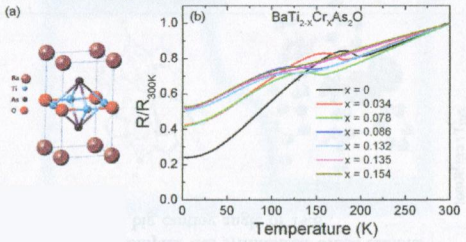

13093 DOI: 10.1021/ic5022559

Thermodynamic N-Donor trans Influence in Labile Pseudo-Octahedral Zinc Complexes: A Delusion?

Lilit Aboshyan-Sorgho, Timothée Lathion, Laure Guénée, Céline Besnard, and Claude Piguet*

Quantifying the thermodynamic trans influence for $d^{10}s^0$ zinc(II) complexes in solution reveals H/S compensation originating from solvation processes, which favor the formation of the statistically penalized facial isomer at low temperature.

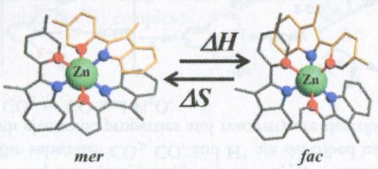

13105 S

DOI: 10.1021/ic502274b

Synthesis, Structure, and Antiproliferative Activity of Ruthenium(II) Arene Complexes with N,O-Chelating Pyrazolone-Based β-Ketoamine Ligands

Riccardo Pettinari,* Fabio Marchetti, Claudio Pettinari, Agnese Petrini, Rosario Scopelliti, Catherine M. Clavel, and Paul J. Dyson

Novel ruthenium half-sandwich complexes containing (N,O)-bound pyrazolone-based β-ketoamine ligands have been prepared and structurally characterized. The complexes show moderate cytotoxicity, one of them being more cytotoxic than cisplatin in the A2780cisR cell line.

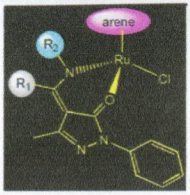

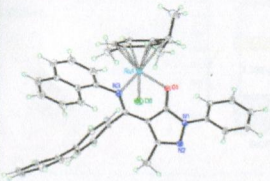

13112 S

DOI: 10.1021/ic5023054

The Conformational Flexibility of the Tetradentate Ligand ^{tBu}N4 is Essential for the Stabilization of (^{tBu}N4)Pd^{III} Complexes

Julia R. Khusnutdinova, Nigam P. Rath, and Liviu M. Mirica*

Cyclic voltammetry, differential pulse voltammety, and spectroelectrochemical studies, as well as CV digital simulations, were performed for a series of Pd^{II} and Pd^{III} complexes that are supported by the flexible multidentate ligand ^{tBu}N4 and that adopt various conformational states in solution ranging from (κ^2-^{tBu}N4)Pd to (κ^3-^{tBu}N4)Pd and (κ^4-^{tBu}N4)Pd. Overall, the coordination to the Pd center of each axial amine donor of ^{tBu}N4 leads to a lowering of the Pd$^{II/III}$ oxidation potential by ~0.6 V.

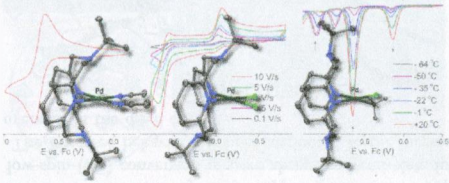

13130 S

DOI: 10.1021/ic502321v

Planar {Ni$_6$} Cluster-Containing Polyoxometalate-based Inorganic–Organic Hybrid Compound and Its Extended Structure

Xingquan Wang, Shuxia Liu,* Yiwei Liu, Danfeng He, Ning Li, Jun Miao, Yujuan Ji, and Guoyu Yang*

Two {Ni$_6$}-containing hybrid compounds have been synthesized under hydrothermal conditions. **1** is an isolated structure based on Dawson-type POMs; **2** is a 3D hybrid formed by introducing succinic acid into the above system. The magnetic properties of them are similar, and the adsorption properties of **2** are also investigated.

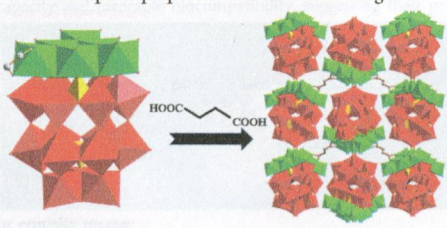

13136 DOI: 10.1021/ic502323w

Efficient Light Harvesting and Energy Transfer in a Red Phosphorescent Iridium Dendrimer

Yang-Jin Cho, Seong Ahn Hong, Ho-Jin Son,* Won-Sik Han,* Dae Won Cho,* and Sang Ook Kang*

A series of red phosphorescent iridium dendrimers were prepared. The harvesting photons on the dendrons followed by efficient energy transfer to the iridium center resulted in high red emissions at 600 nm by metal-to-ligand charge transfer. The intensity of the phosphorescence gradually increased with increasing dendrimer generation. On the basis of the fluorescence quenching rate constants of the dendrons, the energy-transfer efficiencies for **Ir-G$_1$**, **Ir-G$_2$**, and **Ir-G$_3$** were quantitative, and their energy-transfer mechanism was a Förster-type energy transfer. Finally, the light-harvesting efficiencies for **Ir-G$_1$**, **Ir-G$_2$**, and **Ir-G$_3$** were determined.

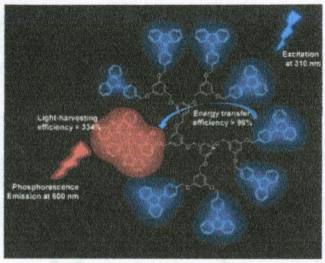

13142 DOI: 10.1021/ic5023517

A Series of Uranium (IV, V, VI) Tritylimido Complexes, Their Molecular and Electronic Structures and Reactivity with CO_2

Anna-Corina Schmidt, Frank W. Heinemann, Laurent Maron, and Karsten Meyer*

A series of uranium tritylimido and tritylamido complexes in oxidation states ranging from +IV to +VI and with homologous core structures were interrogated by XRD analyses, magnetochemical and spectroscopic studies, and DFT computational analysis. The series of structurally very similar complexes over a range of oxidation states provides a unique opportunity to study the electronic properties and to probe the reactivity of the U≡NR/U=N(H)R functional group solely as a function of electron count.

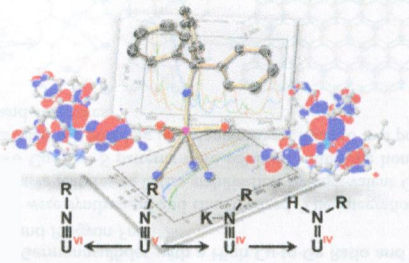

13154 DOI: 10.1021/ic5023467

Synthesis, Structure, and Magnetism of a Family of Heterometallic {Cu_2Ln_7} and {Cu_4Ln_{12}} (Ln = Gd, Tb, and Dy) Complexes: The Gd Analogues Exhibiting a Large Magnetocaloric Effect

Stuart K. Langley, Boujemaa Moubaraki, Corrado Tomasi, Marco Evangelisti,* Euan K. Brechin, and Keith S. Murray*

The syntheses, structures, and magnetic properties of two heterometallic Cu^{II}–Ln^{III} (Ln^{III} = Gd, Tb, and Dy) families, utilizing triethanolamine and carboxylate ligands, are reported. {$Cu^{II}_2Gd^{III}_7$} and {$Cu^{II}_4Gd^{III}_{12}$} complexes display a large magnetocaloric effect, with entropy changes $-\Delta S_m$ = 34.6 and 33.0 J kg^{-1} K^{-1} at T = 2.7 and 2.9 K, respectively, for a 9 T applied field change. A {$Cu^{II}_4Dy^{III}_{12}$} complex displays single-molecule magnet behavior, with an anisotropy barrier to magnetization reversal of 10.1 K.

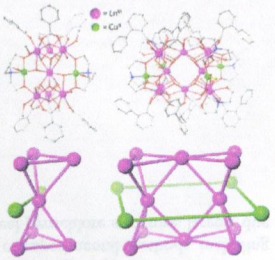

13162 S DOI: 10.1021/ic502381m

Influence of Selenocyanate Ligands on the Transition Temperature and Cooperativity of bapbpy-Based Fe(II) Spin-Crossover Compounds

Sipeng Zheng, Maxime A. Siegler, Olivier Roubeau, and Sylvestre Bonnet*

Eight new molecular iron(II) compounds $[Fe(R_2bapbpy)(NCSe)_2]$ are described, five of which show spin-crossover properties. The selenocyanate axial ligands increase the transition temperatures in these complexes, compared to the previously described thiocyanate analogues $[Fe(R_2bapbpy)(NCS)_2]$. One of the five bis(selenocyanato) SCO compounds is more cooperative than its thiocyanato analogue. The influence of sulfur replacement by selenium on the cooperativity of the spin crossover is discussed.

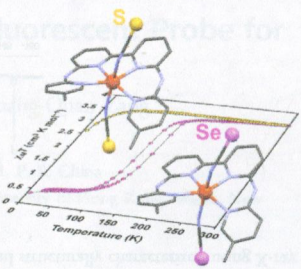

13174 S DOI: 10.1021/ic502365h

Magnetic Properties and Electronic Structures of Ar_3U^{IV}–L Complexes with Ar = $C_5(CH_3)_4H^-$ or $C_5H_5^-$ and L = CH_3, NO, and Cl

Frédéric Gendron, Boris Le Guennic,* and Jochen Autschbach*

The electronic structures and magnetic properties of the tetravalent uranium complexes $(C_5Me_4H)_3UNO$, $(C_5Me_4H)_3UCl$, $(C_5H_5)_3UCl$, and $(C_5H_5)_3UCH_3$ are investigated by quantum chemical calculations. The results are rationalized with the help of natural orbitals obtained for the spin–orbit-free and spin–orbit states, and with crystal-field models using parameters extracted from the ab initio calculations. The calculated susceptibilities agree reasonably well with experiment. $(C_5Me_4H)_3UNO$ exhibits pronounced multiconfigurational character. All complexes afford U-ligand 5f covalent character.

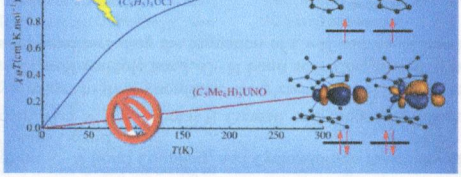

13188 S DOI: 10.1021/ic502410v

Formation of Nanocrystalline Barium Titanate in Benzyl Alcohol at Room Temperature

Sjoerd A. Veldhuis, Wouter J. C. Vijselaar, Tomasz M. Stawski, and Johan E. ten Elshof*

Benzyl alcohol plays a crucial role in the synthesis of nanocrystalline barium titanate (BTO) at temperatures between 23 and 78 °C. The phenylmethoxy ligand of the parent alcohol enhances the reactivity due to steric hindrance of the electronegative phenyl groups and forms a "capping layer" on the as-formed crystallites, inhibiting the growth to a maximum size of 8–10 nm.

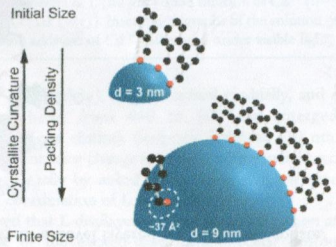

13197 S

DOI: 10.1021/ic502411z

Metastable $(Bi, M)_2(Fe, Mn, Bi)_2O_{6+x}$ (M = Na or K) Pyrochlores from Hydrothermal Synthesis

Luke M. Daniels, Helen Y. Playford, Jean-Marc Grenèche, Alex C. Hannon, and Richard I. Walton*

Crystallization from metal salts in alkali metal hydroxide solution at 200 °C yields two new complex pyrochlore materials whose structures, magnetism, and oxidation-state distribution are reported from a variety of experimental methods, including neutron diffraction and XANES spectroscopy. This suggests some local disorder of the ideal pyrochlore structure, largely due to the presence of A-site Bi^{3+}.

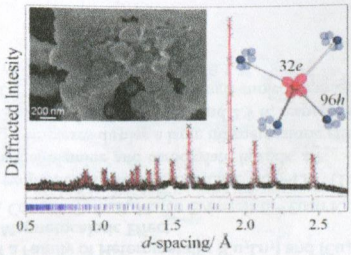

13207 S

DOI: 10.1021/ic502527g

Polymorphic Graphene-like Cuprous Germanosulfides with a High Cu-to-Ge Ratio and Low Band Gap

Qipu Lin, Zhenyu Zhang, Xianhui Bu, and Pingyun Feng*

Three copper-rich germanium sulfides were synthesized and characterized. The integration between heterometallic Ge^{4+} and Cu^{+} in chalcogenides offers dual attractive features of lattice stabilization by high-valent Ge^{4+} and band gap engineering into visible region by low-valent Cu^{+}. Two Cu−Ge−S patterns were achieved within the honeycomb sheet. The decoration of honeycomb sheets by Cu−S chain or their self-coupling into double layers leads to two polymorphic Cu_3GeS_4 configurations with different layer thickness and band structures.

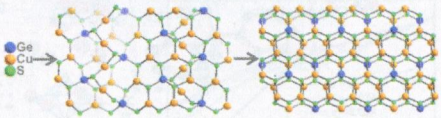

13212 S

DOI: 10.1021/ic502471v

Valence Tautomeric Transitions of Three One-Dimensional Cobalt Complexes

Xiang-Yi Chen, Rong-Jia Wei, Lan-Sun Zheng, and Jun Tao*

Three novel one-dimensional cobalt complexes show solvent-, bridging ligand-, temperature-, and photoinduced valence tautomeric transitions.

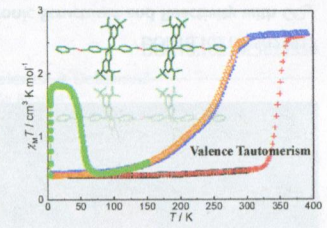

13220 S DOI: 10.1021/ic502473w

A Layered Mixed Zirconium Phosphate/Phosphonate with Exposed Carboxylic and Phosphonic Groups: X-ray Powder Structure and Proton Conductivity Properties

Anna Donnadio, Morena Nocchetti, Ferdinando Costantino, Marco Taddei, Mario Casciola, Fábio da Silva Lisboa, and Riccardo Vivani*

The presence of uncoordinated acidic groups induces a high protonic conductivity in a novel layered zirconium phosphate/phosphonate.

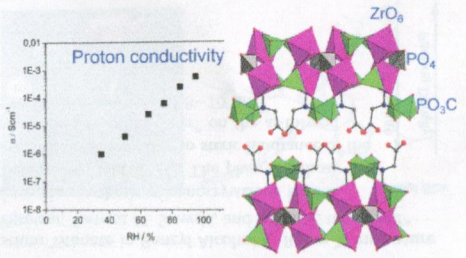

13227 S DOI: 10.1021/ic5026153

Carbon–Hydrogen Bond Activation, C–N Bond Coupling, and Cycloaddition Reactivity of a Three-Coordinate Nickel Complex Featuring a Terminal Imido Ligand

Daniel J. Mindiola,* Rory Waterman, Vlad M. Iluc, Thomas R. Cundari, and Gregory L. Hillhouse*

In addition to presenting synthetic entries to three-coordinate complexes of nickel having a terminally bound imido, we report theoretical studies addressing the Ni=N multiple bond. C–H bond activation as well as reactivity studies with various unsaturated small molecules are reported including the formation of C–N and N–N bonds by coupling reactions.

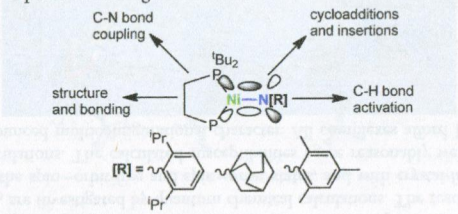

13239 S DOI: 10.1021/ic502617k

Synthesis and Characterization of the Platinum-Substituted Keggin Anion α-$H_2SiPtW_{11}O_{40}^{4-}$

Peter Klonowski, James C. Goloboy, Fernando J. Uribe-Romo, Furong Sun, Lingyang Zhu, Felipe Gándara, Corinne Wills, R. John Errington, Omar M. Yaghi, and Walter G. Klemperer*

Two salts of a platinum-containing silicotungstate Keggin anion have been prepared and structurally characterized using X-ray diffraction and NMR spectroscopic techniques.

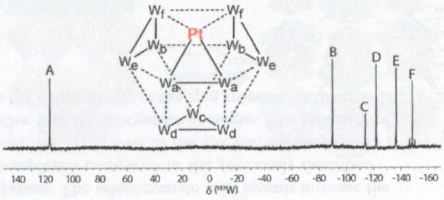

13247 (S) DOI: 10.1021/ic502623t

Enhanced Kinetic Stability of Pure and Y-Doped Tetragonal ZrO_2

Michaela Kogler, Eva-Maria Köck, Stefan Vanicek, Daniela Schmidmair, Thomas Götsch, Michael Stöger-Pollach, Clivia Hejny, Bernhard Klötzer, and Simon Penner*

Pure tetragonal ZrO_2, prepared via a zirconium alkoxide precursor, but without the addition of external stabilizers, shows enhanced kinetic stability in the temperature range $T \leq 400°C$ and persists in the transformation into the monoclinic ZrO_2 polymorph even under moist conditions. This enables for the first time the characterization of its intrinsic structural, electronic, adsorption, and catalytic properties, in comparison to both monoclinic and Y-stabilized ZrO_2.

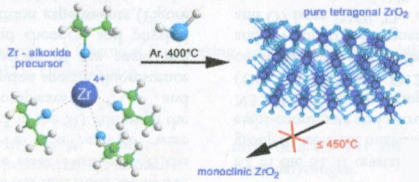

Additions and Corrections

13258 DOI: 10.1021/ic502703a

Correction to Single-Molecule-Magnet Behavior in Mononuclear Homoleptic Tetrahedral Uranium(III) Complexes

Laura C. J. Pereira, Clément Camp, Joana T. Coutinho, Lucile Chatelain, Pascale Maldivi, Manuel Almeida,* and Marinella Mazzanti*

(S) Supporting Information available via online article